A Fully Distributed Heterostructure-Barrier Varactor Nonlinear Transmission-Line Frequency Multiplier and Pulse Sharpener

Ming Li, *Student Member, IEEE*, Kathiravan Krishnamurthi, and Robert G. Harrison, *Member, IEEE*

***Abstract*—The discrete symmetric heterostructure-barrier varactor (HBV) was previously developed as an unbiased frequency-tripling device that needed no second-harmonic idler circuit. Other work investigated nonlinear transmission lines (NLTL's) employing discrete varactors attached to linear guiding structures. Fully distributed Schottky-varactor NLTL's were excessively lossy. This paper explores NLTL's based on *fully distributed HBV structures*. Using both a modified finite-difference time-domain method and numerical integration, it is shown that such NLTL's can provide efficient tripling over a wider input bandwidth than is possible with fixed-tuned triplers. It is also demonstrated that the nonlinearity is strong enough for the NLTL to act as a pulse-sharpening device.**

***Index Terms*— Frequency multiplier, nonlinear transmission line, pulse sharpener, heterostructure barrier varactor.**

I. Introduction

A CLASS of varactors with symmetrical $C(v)$ and antisymmetrical $i(v)$ characteristics was developed previously [1]–[7]. These heterostructure-barrier varactors (HBV's) consist of a thin barrier made of large-bandgap material sandwiched between thick layers of smaller bandgap material. Exploitation of the even $C(v)$ symmetry yields high-power frequency multipliers [4], [8] whose microwave and millimeter-wave output spectra contain only odd-order harmonics. The maximum reactive nonlinearity occurs at zero bias, obviating any need for bias circuits.

Efficient multipliers require HBV's with large capacitance modulation ratios $C_{\max}/C_{\min}$ and small leakage currents. Due to excessive current leakage, early HBV's fabricated on GaAs [1], [2] and InP [3] were found to have poor Q. The resulting triplers had low conversion efficiency ($\eta<5\%$) as well as low output power ($P_{\text{out}}\sim 2$ mW) and exhibited output power saturation at low input power levels. These shortcomings can be overcome by using the improved high-Q stacked HBV structure described in [4]. To achieve high-Q HBV structures, it is found that the design of the current-blocking barriers is critical. The InGaAs/InAlAs system provides effective current blocking as well as low-resistance contacts [5].

The power-handling capability of a varactor multiplier can be improved by adopting the stacked-varactor technique [5], [6]. With n stacked varactors, the output power capability increases as n^2, while the capacitance decreases as n. Simultaneously, power limitations due to RF current saturation are diminished [4]. A tuned (nondistributed) three-stack HBV tripler had a measured efficiency of 20% for an output of 100 mW at 39 GHz [4].

Other work investigated nonlinear transmission lines (NLTL's) consisting of conventional transmission lines periodically loaded with discrete varactors [7]. NLTL's consisting of fully distributed Schottky-barrier varactor structures were too lossy [7].

Here we explore the feasibility of fully distributed NLTL's that use an extended version of the HBT structure with the improved features described above. To evaluate the performance, we obtain a differential equivalent circuit for the distributed device, from which we derive a nonlinear wave equation. The finite-difference time-domain (FDTD) method is then applied to this wave equation, using appropriate initial and boundary conditions. As a check, the NLTL is also modeled directly using Libra[1] and the transient solution obtained by integration in the time domain. The time-domain waveforms and frequency-domain spectra obtained by the two methods are in excellent agreement.

The simulations demonstrate that such NLTL's can provide efficient tripling over a wider range of input frequencies than is possible with fixed-tuned triplers, and that they can also act as frequency quintuplers. Furthermore, it is shown that the reactive nonlinearity of the distributed HBV is sufficient for the NLTL to act as a useful pulse-sharpening device.

II. Device Model and Wave Equation

The composition and geometry of the pseudomorphic MBE layers for the typical triple-stacked HBV shown in Fig. 1(a) are similar to those in [5]. The idea is to extend the HBV device in one of its "horizontal" dimensions to form a fully distributed NLTL, see Fig. 1(b). At the high frequencies for which it is well suited, such an NLTL would be of the order of $\sim$1 mm long and a few tens of micrometers wide. The effective height of the line is the distance between the highly doped

Manuscript received March 27, 1998; revised August 27, 1998. The work of M. Li and R. G. Harrison was supported by the Natural Sciences and Engineering Research Council of Canada under Grant OGP 1340.

M. Li is with the Department of Electronics, Carleton University, Ottawa, Ont., Canada K1S 5B6 and PlainTree Systems Inc., Ottawa, Ont., Canada.

K. Krishnamurthi is with Nortel Labs, Nepean, Ont., Canada, K2G 6J8.

R. G. Harrison is with the Department of Electronics, Carleton University, Ottawa, Ont., Canada K1S 5B6.

Publisher Item Identifier S 0018-9480(98)09205-9.

[1] Libra 6.0, Hewlett-Packard Company, Santa Rosa, CA, 1995.

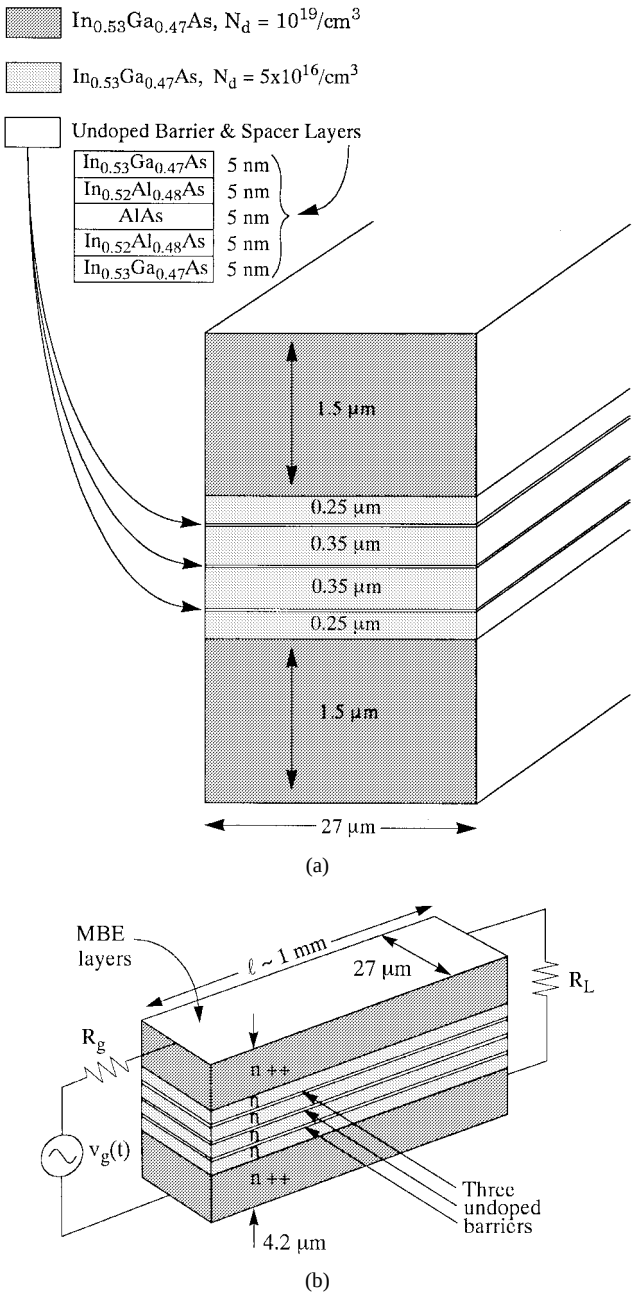

Fig. 1. (a) Composition and geometry of pseudomorphic layers for a typical triple-stacked fully distributed heterostructure-barrier transmission line. (b) The distributed HBV NLTL connected to source and load.

layers, about 1.2 μm in the case of Fig. 1. The concept of "characteristic impedance" is, of course, meaningless for such a transmission line, because of its highly nonlinear distributed capacitance.

A. Modeling the NLTL

Fig. 2 shows an equivalent circuit for an infinitesimal section of the NLTL. Here, $i(z,t)$ is the instantaneous total current entering a section of length dz at location z and time instant t, while $v(z,t)$ is the corresponding instantaneous voltage between the top and bottom highly doped regions of the HBV structure, represented in the model as good conductors. L_z is the inductance/length (H/m), and $q_z(v)$ is the charge/length

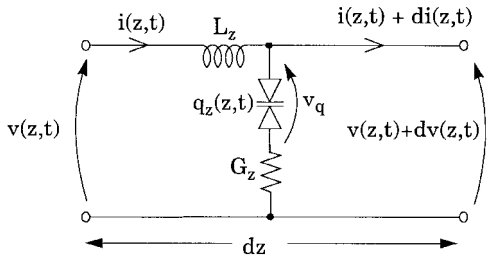

Fig. 2. Equivalent circuit of an infinitesimal section of length dz of the distributed nonlinear transmission line.

(C/m) on the NLTL. G_z is a conductance/length (S/m) that models the resistance of the undepleted part of the bulk HBV material. (The corresponding series resistance in discrete varactors is usually denoted R_s).

Following [9], the quantities q_z and v_q, the voltage across the "ideal" charge store in Fig. 2, are assumed to be related by the empirical cubic expression

$$\alpha v_q(z,t) = \frac{q_z(z,t)}{q_{z0}} + \beta\left(\frac{q_z(z,t)}{q_{z0}}\right)^3 \tag{1}$$

where α, β, and q_{z0} are constants depending on the HBV structure and material. This $q(v)$ characteristic and the corresponding small-signal voltage-dependent $C(v)$ characteristic are depicted in Fig. 3.

B. Nonlinear Wave Equation

Application of Kirchhoff's voltage law to the infinitesimal section of Fig. 2 yields the voltage drop across the inductive element $L_z dz$

$$dv(z,t) = \frac{\partial v(z,t)}{\partial z}dz = -L_z\frac{\partial i(z,t)}{\partial t}dz \tag{2}$$

and Kirchhoff's current law leads to

$$di(z,t) = \frac{\partial i(z,t)}{\partial z}dz = -\frac{\partial q_z(z,t)}{\partial t}dz. \tag{3}$$

Eliminating i and v between (2) and (3), there results a relation between v and q_z

$$\frac{\partial^2 v}{\partial z^2} = L_z\frac{\partial^2 q_z}{\partial t^2}. \tag{4}$$

Also, using Ohm's law on the shunt branch

$$v + dv = v_q - \frac{1}{G_z}\frac{di}{dz}. \tag{5}$$

Eliminating v between (4) and (5), and using (1) to eliminate v_q, there results a nonlinear wave equation for the normalized charge/length $x(z,t)$

$$\frac{\partial^2}{\partial z^2}[x + \beta x^3] + \xi\frac{\partial^3 x}{\partial z^2 \partial t} = \frac{1}{u^2}\frac{\partial^2 x}{\partial t^2} \tag{6}$$

where $x(z,t) = q_z(z,t)/q_{z0}, u = 1/\sqrt{(C_{z0}L_z)}$ has the dimensions of velocity (m/s), $C_{z0} = \alpha q_{z0}$ is the capacitance/length (F/m) at zero bias, and $\xi = \alpha q_{z0}/G_z = C_{z0}/G_z$ (s) is a loss parameter. This wave equation, which incorporates a cubic nonlinearity, forms the basis of the simulation procedure.

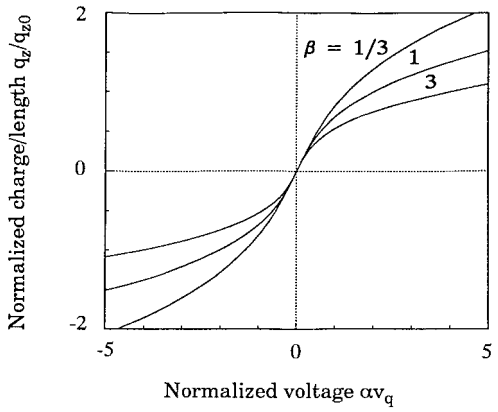

(a)

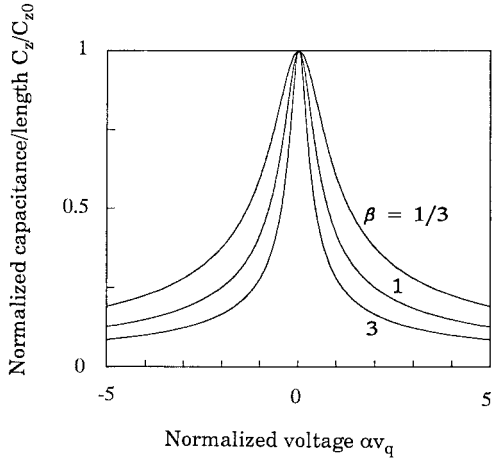

(b)

Fig. 3. (a) The empirical charge/length versus voltage characteristic $q_z(v_q)$ for the distributed HBV, as given by the inverse of (1), for three values of β. (b) The corresponding capacitance/length versus voltage characteristic $C_z(v_q)$.

III. Simulation Approaches

Realistic simulations of the NLTL are carried out using two different approaches: 1) a modified FDTD method and 2) numerical integration.

A. The Modified FDTD Method

The FDTD and transmission-line matrix (TLM) methods have previously been combined in order to simulate the time-domain response of a nonlinear device [10] or a transmission line [11]. The advantages of this approach are that the TLM provides a physical basis for wave propagation, while the FDTD offers computational efficiency.

The algorithm used here is similar to that in [10]. The difference is that instead of Maxwell's curl equations, we use the nonlinear partial differential equation (6) to describe the wave propagation. Whereas general FDTD or TLM methods require six field variables, three for $\mathbf{E}$ and three for $\mathbf{H}$, our algorithm needs only one variable: the normalized charge $x(z,t)$. Consequently, our algorithm is much less computer-intensive than general FDTD or TLM methods. Furthermore, use of an empirical charge-voltage relationship such as (1)

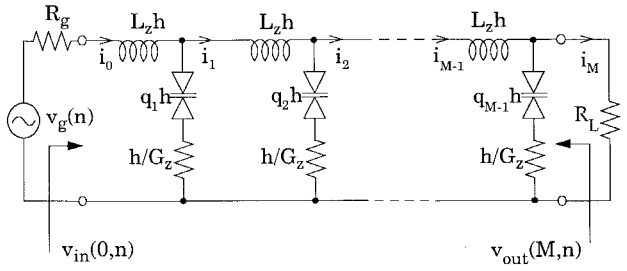

Fig. 4. The discretized equivalent circuit of the NLTL.

makes it easy to incorporate additional linear or nonlinear elements into the equivalent circuit for the NLTL, as required.

Applying FDTD [12] to the wave equation (6), we obtain in the lossless[2] case ($\xi = 0$) the iteration

$$\begin{aligned} x_{i,n+1} = {} & 2x_{i,n} - x_{i,n-1} \\ & + \left(\frac{ku}{h}\right)^2 (x_{i-1,n} - 2x_{i,n} + x_{i+1,n})\left(1 + 3\beta x_{i,n}^2\right) \\ & + \frac{3}{2}\left(\frac{ku}{h}\right)^2 \beta x_{i,n}(x_{i+1,n} - x_{i-1,n})^2. \end{aligned} \tag{7}$$

In (7), the normalized charge $x(z,t)$ is discretized in space and time as

$$x_{i,n} = x(ih, nk) \tag{8}$$

where $h = \Delta z$ and $k = \Delta t$ are the space and time increments, and i and n are integers.

Fig. 4 shows a discretized NLTL equivalent circuit consisting of a finite number M of separate subsections. Each subsection contains a lumped inductance L_zh (H) and a nonlinear discrete HBV storing a charge q_zh (C). The boundary conditions for the circuit are represented as

$$v_{in}(0,n) = v_g(n) - i_0 R_g \tag{9}$$

$$v_{\text{out}}(M,n) = i_M R_L. \tag{10}$$

The physical length of the NLTL is $l = Mh$.

Application of Kirchhoff's current law and FDTD [12] to Fig. 4 results in

$$\begin{aligned} i_0 &= i_1 + q_{z0}h\frac{x_{1,n} - x_{1,n-2}}{2k}, \\ i_1 &= i_2 + q_{z0}h\frac{x_{2,n-1} - x_{2,n-3}}{2k} \\ &\vdots \\ i_M &= i_{M-1} + q_{z0}h\frac{x_{M-1,n} - x_{M-1,n-2}}{2k} \\ i_{M-1} &= i_{M-2} + q_{z0}h\frac{x_{M-2,n-1} - x_{M-2,n-3}}{2k} \\ &\vdots \end{aligned} \tag{11}$$

Combining (9) and (10) with (1), the boundary and initial conditions can be satisfied.

[2] In the full simulations, the loss parameter ξ is included ($G_z < \infty$).

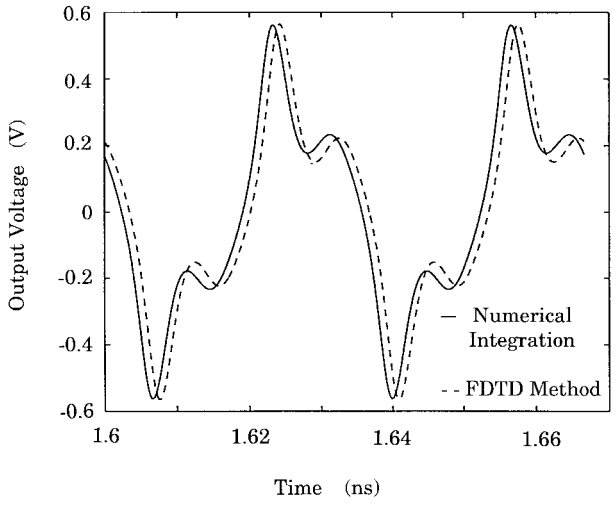

Fig. 5. Comparison of the output waveforms predicted by the two simulation methods. —— Numerical integration; --- FDTD method.

B. Numerical Integration Approach

The other approach to simulating the NLTL is by numerical integration, as implemented in Libra 6.0.[1] The procedure adopted is as follows.

1) Do curve fitting in order to represent the $C(v)$ relationship implied in (1) by the polynomial

$$C(v) = c_0 + c_1 + c_2 v^2 + \cdots + c_m v^m. \qquad (12)$$

Note that $C(v) = dq_z/dv$ and that the coefficients $c_0, c_1, c_2, \cdots, c_m$ depend on the constants a, b, and q_{z0}. The number of coefficients used here was $m \sim 20$.

2) Use (12) as the nonlinear capacitor model in Libra, and build the equivalent circuit of the NLTL.
3) Do time-domain simulations using the "Transient Bench" numerical integration procedure of Libra 6.0.

IV. Frequency-Multiplier Simulations

A. Comparison of Simulation Methods

Fig. 5 compares the NLTL output voltage waveforms as predicted by the two methods when the input signal is a 30-GHz sinewave of amplitude 1.0 V. Here $M = 25$ sections were used in the equivalent circuit of Fig. 4. Each subsection is equivalent to a discrete HBV of area 27×27 $(\mu\text{m})^2$ [5], so that the width of the simulated NLTL is 27 μm, and its overall length is $l = 25 \times 27\,\mu\text{m} = 0.67$ mm. Utilizing the data in [5], the parameters of each such subsection were taken to be $\alpha = 1.0$, $\beta = 3.0$, $L_z h = 0.05$ nH, $C_{z0} h = 0.1$ pF, $h/G_z = 1.0\,\Omega$. The generator and load resistors R_g and R_L were each set to 50 Ω. Fig. 5 shows good agreement between the FDTD and numerical-integration simulations.

The FDTD and numerical-integration methods are both CPU-time efficient compared with general FDTD or TLM. The FDTD simulations run about twice as fast as the Libra simulations, but this advantage is more than offset by the detailed set-up files required for the FDTD runs. The remainder of the results reported here were therefore obtained from Libra simulations.

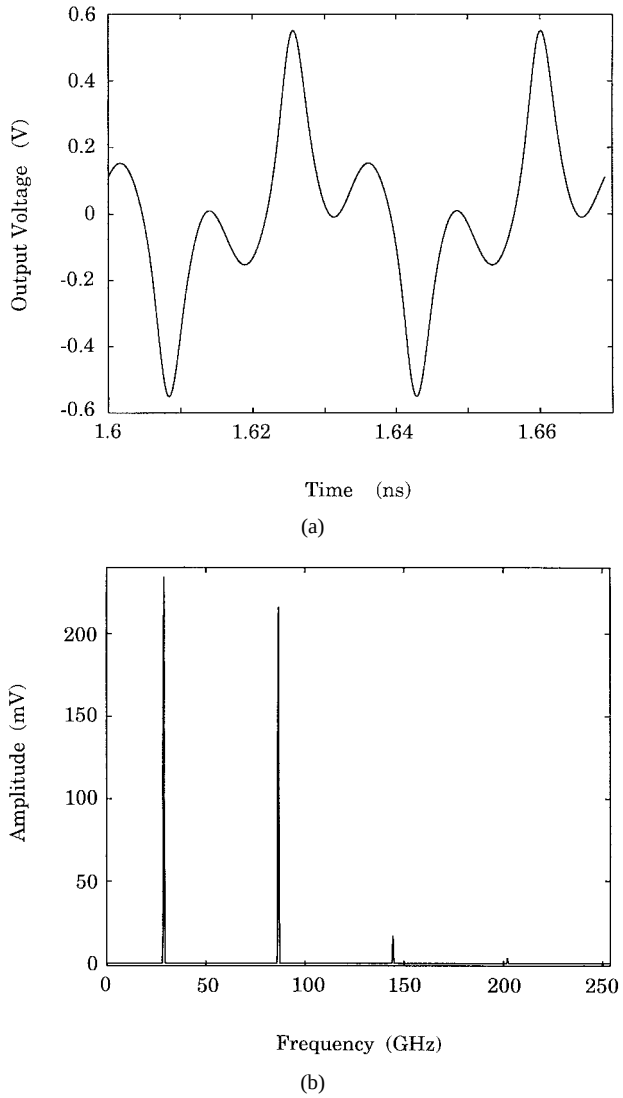

Fig. 6. Tripler action when the NLTL length is $l = 1.35$ mm ($M = 50$ subsections), the input frequency is $f_{\text{in}} = 29$ GHz, and the input power is $P_{\text{in}} = 4$ dBm. (a) The output voltage waveform. (b) The output voltage spectrum.

B. Modes of Multiplier Operation

To investigate the behavior of the distributed frequency multiplier for different input frequencies f_{in}, we assumed a 50-section NLTL (overall length $l = 1.35$ mm) with the following per-section parameters: $\alpha = 1.0$, $\beta = 3.0$, $L_z h = 0.05$ nH, $C_{z0} h = 0.1$ pF, and $h/Gz = 0.5\,\Omega$. Fig. 6(a) shows the simulated output waveform when $f_{\text{in}} = 29$ GHz ($f_{\text{out}} = 87$ GHz). Fig. 6(b) is the corresponding spectrum, showing good operation as a tripler, with a third-harmonic-to-fundamental power ratio of -0.28 dB. Under this condition the conversion loss is 5.1 dB. Note that all even harmonic generation is *suppressed* by the symmetrical $C(v)$ of the HBV structure, contributing to the overall efficiency of the frequency-conversion process.

Fig. 7(a) depicts the output waveform when f_{in} is reduced to 20 GHz ($f_{\text{out}} = 60$ GHz): higher-harmonic components are now evident. The corresponding spectrum in Fig. 7(b) shows that the amplitude of the fifth harmonic is now larger than

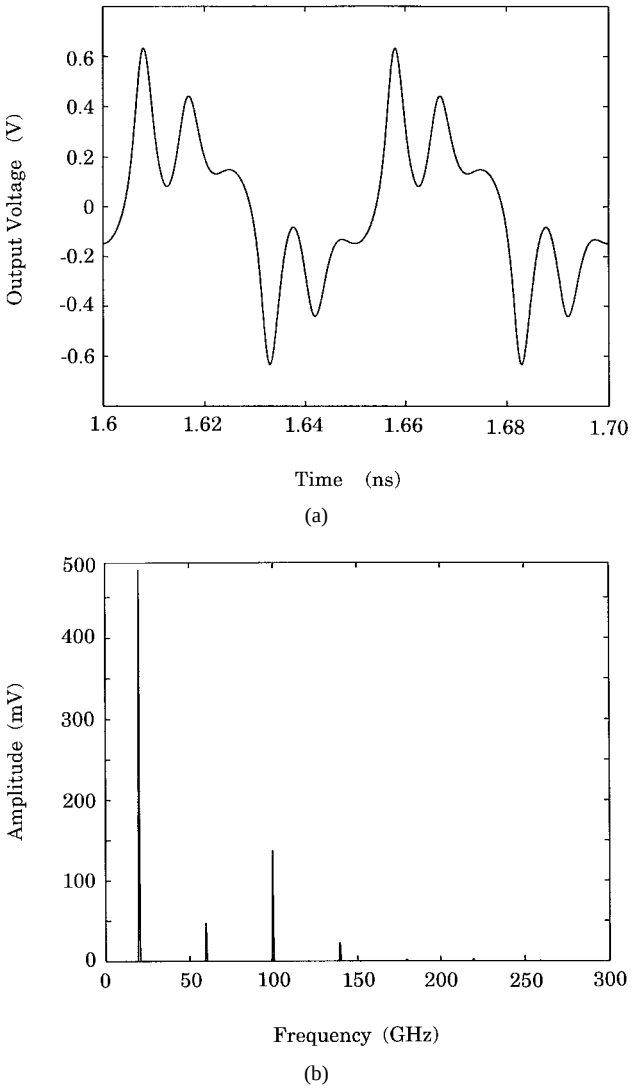

Fig. 7. Quintupler action when the NLTL length is $l = 1.35$ mm ($M = 50$ subsections), the input frequency is $f_{\rm in} = 20$ GHz, and the input power is $P_{\rm in} = 4$ dBm. (a) The output voltage waveform. (b) The output voltage spectrum.

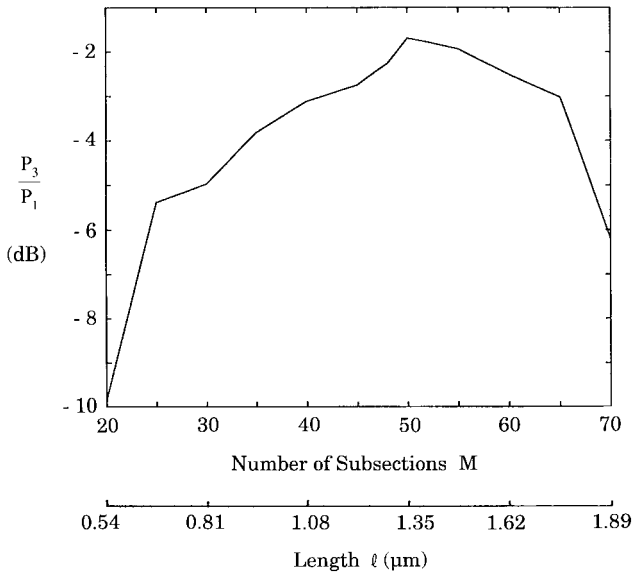

Fig. 8. Ratio of the third-harmonic output power P_3 to the fundamental power P_1 as a function of the NLTL length l. The input frequency is fixed at $f_{\rm in} = 30$ GHz.

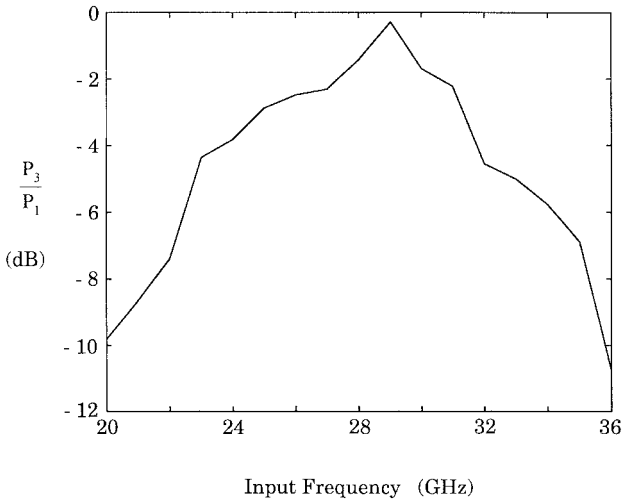

Fig. 9. Ratio of the third-harmonic output power P_3 to the fundamental power P_1 as a function of the input frequency $f_{\rm in}$ when $l = 1.35$ mm ($M = 50$ subsections).

the third, and that the NLTL is now operating as a frequency quintupler.

C. Multiplier Optimization

As a preliminary optimization of the NLTL tripler, the following procedure was adopted.

1) Set $f_{\rm in} = 30$ GHz and vary the number of sections (in the equivalent circuit of Fig. 4) over the range $20 \leq M \leq 70$.
2) Set $M = 50$ sections and vary the input frequency over the range $20 \leq f_{\rm in} \leq 30$ GHz.

Fig. 8 shows the result of experiment 1). It is seen that for $f_{\rm in} = 30$ GHz, the optimum M is 50, yielding a power ratio of -1.69 dB (compared with the -0.28 dB obtained for $f_{\rm in} = 29$ GHz). The power ratio remains better than -3.0 dB over a range of NLTL lengths corresponding to $40 \leq M \leq 60$ sections.

Fig. 9 gives the result of varying $f_{\rm in}$. Here it is found that the effective 3-dB bandwidth corresponds to input frequencies in the range 25–35 GHz, with output frequencies covering the 75–105 GHz band.

D. Comments

1) In both Figs. 6(a) and 7(a) there is evidence of the generation of solitons of ~4 ps width at half-height [13].
2) In the frequency-multiplying mode, the absence of even-harmonic generation
   a) simplifies the output filtering;
   b) improves the conversion efficiency, since less power is going into unwanted harmonics.

V. Pulse-Sharpening Simulations

In addition to investigating the frequency-multiplying properties of the HBV NLTL, Libra simulations were done to

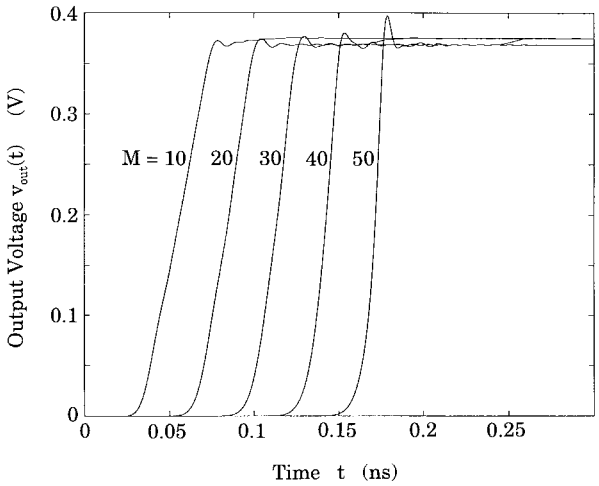

Fig. 10. Pulse responses of HBV NLTL's of lengths $0.27 \leq l \leq 1.35$ mm ($10 \leq M \leq 50$ subsections) to a "slow" input pulse $v_g(t)$ of risetime 50 ps and amplitude 0.75 V.

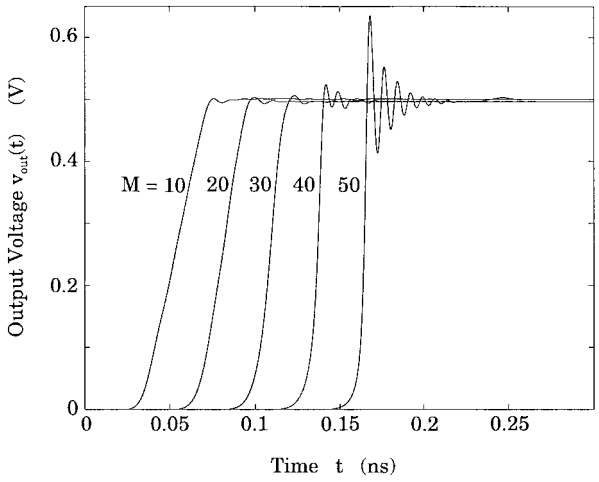

Fig. 11. Same as Fig. 10, but input pulse $v_g(t)$ has amplitude 1.0 V.

determine its response to input pulses. The parameters assumed for the HBV structure were the same as those for the multiplier simulations: $\alpha = 1.0$, $\beta = 3.0$, $L_z h = 0.1$ nH, $C_{z0} h = 0.1$ pF, and $h/Gz = 0.5\,\Omega$.

A. Numerical Pulse-Sharpening Experiments

Fig. 10 shows the result of applying a "slow" step input pulse $v_g(t)$ of amplitude 0.75 V, and risetime $t_r = 50$ ps, when the line length l is increased from zero to 1.35 mm (50 subsections).[3] It is seen that the rising pulse edge becomes progressively steeper as the NLTL length is increased. When the length reaches 1.08 μm ($M = 40$ subsections) the output pulse $v_{\text{out}}(t)$ has been "sharpened" dramatically, so that its 10–90% risetime is reduced to $\sim$16 ps. Thereafter, "ringing" sets in. It is found that the optimum NLTL length for good pulse sharpening (fast risetime without excessive ringing) is $l \sim 1.22\,\mu$m ($M = 45$ subsections) for the chosen set of parameters.

In Fig. 11, the step amplitude is increased to 1.0 V, while the NLTL length is varied over the same range as before. The pulse response is now more oscillatory, and the risetime is even further reduced to $\sim$7.5 ps when $l \sim 1.22\,\mu$m. The change in the character of the response as the input amplitude is increased is not unexpected in view of the strong reactive nonlinearity of the HBV NLTL.

B. Comments

1) The pulse-sharpening effect is due to the fact that the voltage-dependent (small-signal) propagation velocity on the NLTL is

$$u(v) = 1\sqrt{C_z(v) L_z}.$$

Since C_z decreases with $|v|$, see Fig. 3(b), the small-amplitude part of the pulse propagates faster than the large-amplitude part.

2) In the pulse-sharpening mode, the high-frequency performance is not limited by the Bragg cutoff-frequency effect, as it is in conventional periodic NLTL structures [13].
3) The full electrical symmetry of the HBV NLTL allows both positive-going and negative-going pulse edges to be sharpened. In contrast, with conventional asymmetric Schottky-varactor NLTL's, only a single polarity of pulses can be sharpened because the other polarity would drive the Schottky varactors into forward bias.
4) Again, there is evidence of the generation of solitons of width $\sim$4 ps.

[3] The output pulse height is $\sim$0.375 V because of the 50-Ω terminations.

VI. Conclusions

A fully distributed NLTL incorporating an extended HBV structure is reported. Nonlinear transient analysis is carried out using both FDTD and numerical integration methods. The results indicate that this new device is promising as an *untuned* wideband frequency multiplier for millimeter-wave communications. The pulse-response analyses show that the HBV NLTL is also very promising as a high-speed bilateral pulse-sharpening device.

Further work will be directed: 1) to optimizing the parameters of the NLTL and its embedding circuits for efficient harmonic generation for specified output power levels and bandwidths and 2) to optimizing it as a high-speed pulse-enhancing device.

References

[1] A. Rydberg, H. Grönqvist and E. L. Kollberg, "Millimeter and submillimeter-wave multipliers using quantum barrier varactor (QBV) diodes," *IEEE Electron Device Lett.*, vol. 11, pp. 373–375, Sept. 1990.
[2] H. X. Liu, L. B. Sjøgren, C. W. Domier, N. C. Luhmann, D. L. Sivco, and A. Y. Cho, "Monolithic quasioptical frequency tripler array with 5 W output power at 99 GHz," *IEEE Electron Device Lett.*, vol. 14, pp. 329–331, July 1993.
[3] A. V. Räisänen, T. J. Tolmunen, M. Natzic, M. A. Frerking, E. Brown, H. Grönqvist, and S. M. Nilsen, "A single barrier varactor quintupler at 170 GHz," *IEEE Microwave Theory Tech.*, vol. 43, pp. 685–688, Mar. 1995.
[4] K. Krishnamurthi and R. G. Harrison, "Millimeter-wave frequency tripling using stacked heterostructure-barrier varactors on InP," *IEE*

Proc.—Microwaves, Antennas and Propagation, vol. 143, pp. 272–276, Aug. 1996.
[5] K. Krishnamurthi, "Heterostructure varactors on InP and GaAs for millimeter-wave frequency triplers," Ph.D. dissertation, Carleton Univ., Ottawa, Canada, Jan. 1995.
[6] A. Rahal, E. Boch, C. Rogers, J. Ovey, and R. G. Bosisio, "Planar multi-stack quantum barrier varactor tripler evaluation at W-band," *IEE Electron. Lett.*, vol. 31, pp. 2022–2023, Nov. 1995.
[7] H. Shi, W. M. Zhang, C. W. Domier, N. C. Luhmann, L. B. Sjøgren, and H. X. Liu, "Novel concepts for improved nonlinear transmission line performance," *IEEE Trans. Microwave Theory Tech.*, vol. 43, pp. 780–789, Apr. 1995.
[8] R. J. Baker, D. J. Hodder, B. P. Johnson, P. C. Subedi, and D. C. Williams, "Generation of kilovolt-subnanosecond pulses using a nonlinear transmission line," *Meas. Sci. Technol.*, vol. 4, pp. 893–895, Aug. 1993.
[9] K. Krishnamurthi and R. G. Harrison, "Analysis of symmetric-varactor frequency triplers," in *IEEE Int. Microwave Symp. Dig.*, June 1993, pp. 649–652.
[10] R. H. Voelker and R. J. Lomax, "A finite-difference transmission-line matrix method incorporating a nonlinear device model," *IEEE Trans. Microwave Theory Tech.*, vol. 38, pp. 302–312, Mar. 1990.
[11] J. Xu and J. M. Chuang, "Modeling of nonlinear-optical media with the TLM-based finite-difference-time-domain method," *Microwave Opt. Technol. Lett.*, vol. 13, pp. 259–264, Dec. 1996.
[12] R L. Ketter, *Modern Methods of Engineering Computation*. New York: McGraw-Hill, 1969.
[13] E. Carman, K. Giboney, M. Case, M. Kamegawa, R. Yu, K. Abe, M. J. W. Rodwell, and J. Franklin, "28–39 GHz distributed harmonic generation on a soliton nonlinear transmission line," *IEEE Microwave Guided Wave Lett.*, vol. 1, pp. 28–31, Feb. 1991.
[14] M. Li and R. G. Harrison, "A fully-distributed heterostructure-barrier-varactor nonlinear-transmission-line frequency tripler," in *IEEE Int. Microwave Symp. Dig.*, June 1998, pp. 1639–1642.
[15] D. Jäger, private communication, 1998.

Ming Li (S'96) received the Masters degree in electrical engineering from Tianjin University, Tianjin, China, in 1989.

She taught at Tianjin University from 1990 to 1994. She became a Research Associate in the Department of Electronics, Carleton University, Ottawa, Ont., Canada, in 1994. Since then she has worked in several different RF circuit design and application areas and has published papers on microwave circuit modeling, MMIC amplifier antenna design, and millimeter wave tripler modeling and optimization. She is now completing a thesis part-time at Carleton University, while working full-time as an ASIC Design Engineer at PlainTree Systems Inc., Ottawa, Canada, where she is working on gigabit Ethernet switches.

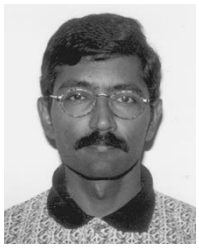

Kathiravan Krishnamurthi was born in Coimbatore, Tamil Nadu, India, in 1965. He received the B.E (Hons.) degree from Regional Engineering College, Tiruchirapalli, India, in 1987. He pursued his graduate work in Canada earning the M.Sc. degree from the University of Saskatchewan, Saskatoon, in 1990 and the Ph.D. degree from Carleton University, Ottawa, Canada, in 1995.

From 1987 to 1994 he worked on direct microwave modulation, resonant tunneling diode mixers, and millimeter-wave frequency triplers using heterostructure varactors. He is now with Nortel Wireless Laboratories, Ottawa, Ont., Canada, designing CDMA receiver subsystems and components.

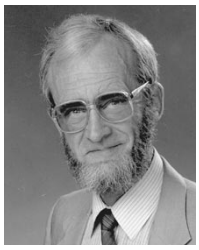

Robert G. Harrison (M'82) received the B.A. and M.A. (Eng.) degrees from Cambridge University, England, in 1956 and 1960, respectively, and the Ph.D. and D.I.C. degrees from the University of London, England, in 1964.

From 1964 to 1976 he was with the Research Laboratories of RCA Ltd., Ste-Anne-de-Bellevue, P.Q., Canada. In 1977 he became Director of Research at Com Dev Ltd., where he worked on nonlinear microwave networks. From 1979 to 1980 he designed spread-spectrum systems at Canadian Marconi Company, Montreal, Quebec. Since 1980 he has been a Professor in the Department of Electronics, Carleton University, Ottawa, Ont., Canada. His research interests include the modeling of nonlinear microwave device/circuit interactions by a combination of analytical and numerical techniques. He has authored or coauthored over 55 technical papers, mostly in the area of nonlinear microwave circuits. He holds a number of basic patents in the area of microwave frequency-division devices.

Dr. Harrison received the "Inventor" award from Canadian Patents and Development in 1978.